Regular Article

PHYSICAL CHEMISTRY RESEARCH
Published by the
Iranian Chemical Society
www.physchemres.org
info@physchemres.org

Phys. Chem. Res., Vol. 9, No. 2, 193-209, June 2021
DOI: 10.22036/pcr.2020.248964.1837

Structural, Spectroscopic (UV-Vis and IR), Electronic and Chemical Reactivity Studies of (3,5-Diphenyl-4,5-dihydro-1*H*-pyrazol-1-yl)(phenyl)methanone

S.L. Dhonnar[a,*], V.A. Adole[b], N.V. Sadgir[a] and B.S. Jagdale[a,b]

[a]*Department of Chemistry, L.V.H. Arts, Science, and Commerce College, Panchavati, Nashik (M.S) India*
[b]*Department of Chemistry, Arts, Science, and Commerce College, Manmad, Dist.-Nashik (MS) India*

(Received 20 September 2020, Accepted 22 December 2020)

(3,5-Diphenyl-4,5-dihydro-1*H*-pyrazol-1-yl)(phenyl)methanone (DPPPM) was synthesized using a rapid and recyclable reaction media of polyethylene glycol-400 (PEG-400) and catalytic amount of acetic acid. This method gives remarkable advantages such as a simple workup and a greener method by avoiding hazardous and toxic solvents. The computational calculations for the title compound were carried out using the density functional theory (DFT) method with B3LYP hybrid functional and 6-311++G(d,p) basis set. The structural parameters like bond lengths, bond angles, and dihedral angles were obtained from the optimized molecular geometry and discussed. This structural analysis shows that the DPPPM molecule has a non-planar structure and possess C1 point group symmetry. The infrared vibrational spectral bands assignments were made by correlating experimental findings with the computed data that showed a good agreement. The electronic spectral properties were explored using the time-dependent DFT in the gas phase and two different polarity solvents. The theoretical UV-Vis absorption results obtained were in an acceptable agreement with the UV-Vis absorption experimental results. The solvent effect on wavelength of absorption was also reported. The frontier molecular orbital, molecular electrostatic surface potential and global chemical reactivity parameters for the title molecule in the gas phase were reported and discussed. Based on the results, the synthesized molecule possesses a good strength and kinetic stability.

Keywords: DFT, FT-IR, UV-Vis, HOMO-LUMO

INTRODUCTION

Chalcones are mainly used as a precursor for the synthesis of pyrazolines. The N-substituted pyrazolines are an important class of biologically active compounds exhibiting a broad spectrum of biological activities. The notable biological spectrum includes COX-2 inhibitors [1], antibacterial [2], antifungal [3], anti-inflammatory [4], analgesic [4,5], antidepressant [6], anticancer [7], anticonvulsant [8], *etc*. They are also used as fluorescent probes [9] in some elaborate chemo sensors and as photosensitizers [10]. Various different strategies for the synthesis of (3,5-diphenyl-4,5-dihydro-1*H*-pyrazol-1-yl)(phenyl)methanone are known. However, many of these methods are associated with various drawback such as tedious experimental workup procedure, harsh reaction condition, unsatisfactory yield, long reaction time and use of hazardous and toxic solvents. Hence, there is a need to develop a rapid and environmentally benign synthetic procedure for the synthesis of title molecule. In the recent years, use of polyethylene glycol (PEG) solvents has become dominant due to several advantages associated with them. The PEG solvents are known to be inexpensive, easily available, thermally stable, recyclable, biologically compatible, and non-toxic [11-12]. Due to these impeccable advantages of PEG solvents, they are used as solvents and catalysts in numerous organic transformations [13-16]. In view of the emerging importance of PEG as reusable and safe reaction media, here, we report the synthesis of (3,5-diphenyl-4,5-dihydro-1*H*-pyrazol-1-yl)(phenyl)methanone

*Corresponding author. E-mail: sunildhonnar@gmail.com

using alternative reaction media polyethylene glycol-400 (PEG 400) with catalytic amount of acetic acid. To the best of our knowledge, there is no any report for the synthesis of (3,5-diphenyl-4,5-dihydro-1*H*-pyrazol-1-yl)(phenyl) methanone by using this reaction medium.

Computational sciences have made easier anticipating the physical, chemical and spectroscopic properties of the small molecules. The properties like optimized structure, bond lengths, and dihedral angles are easily predicted using density functional theory (DFT) computations [17,18]. In addition, UV-Vis, vibrational, NMR and Raman spectral investigations are also explored by means of DFT calculations [19,20]. The B3LYP functional and 6-311++G(d,p) basis set are found to be the most used level of theory in the DFT computations for studying optical, spectral and charge density properties of the large and small molecules [21-24]. Considering all these vital edges and in continuation of our work on DFT studies, (3,5-diphenyl-4,5-dihydro-1*H*-pyrazol-1-yl)(phenyl)methanone was studied using the combined theoretical and experimental viewpoints. The molecular properties like optimized molecular geometry, structural entities, HOMO-LUMO energies, charge distribution, MESP plot, global reactivity parameters and spectroscopic properties have been explored in the present work. Crucially, theoretical spectroscopic data were compared with the experimental results for the assignment of spectral bands.

EXPERIMENTAL

Material and Physical Measurements

All chemicals required for synthesis were obtained from commercial sources (AR grade with purity > 99%) and used without further purification. The melting points were determined in open capillaries and were uncorrected. The purity of the compound was checked by TLC using silica gel-G coated Al-plates and spot visualize under UV radiation. The FT-IR spectrum was recorded on Shimadzu spectrometer on KBr pellets. The ^{1}H NMR spectrum was recorded on a Brucker Advance II 500 MHz spectrometer using TMS as an internal standard. The high-resolution mass spectral investigation was performed using the ESI mode on the Bruker Impact II UHR-TOF MS instrument. The electronic absorption spectrum of the title compound was recorded at room temperature in DCM and DMSO solvents on an Anatech UV-Vis spectrometer working at 200-800 nm.

Synthesis

Synthesis of (2E)-1,3-diphenylprop-2-en-1-one. 5 ml KOH (0.03 mol) solution was added to the equimolar mixture of acetophenone (0.01 mol) and benzaldehyde (0.01 mol) in PEG 400 (15 ml) solvent with constant stirring. After addition of KOH, the reaction mixture was continued stirring at 40-50 °C until the reaction was completed. The completion of the reaction was monitored by TLC. After completion of the reaction, the reaction mixture was worked up with ice-cold water. The separated product was filtered out. The filtrate was evaporated to remove the water content, leaving PEG behind.

Synthesis of (3,5-diphenyl-4,5-dihydro1*H*-pyrazol-1-yl)(phenyl)methanone. A mixture of chalcone 3 (0.01 mol) and benzohydrazide 4 (0.012 mol) was placed in a 100 ml round bottom flask with 10 ml of PEG-400. To this solution, 1 ml of glacial acetic acid was added dropwise with continuous stirring. Then, the reaction mixture was reflux and stirred on a magnetic stirrer at 50-70 °C for about 4-5 h. The reaction progress was monitored by TLC. After completion of the reaction, the reaction mixture was cooled and poured into crushed ice. The precipitate formed was filtered off and recrystallized from isopropanol to give the pure product (Scheme 1).

Yield: 83%, M.P.: 162 °C, UV-Vis (λ_{max}, nm,) DCM: 301; FT-IR (KBr, in cm^{-1}): 3064 (aromatic C-H str.), 2933 (CH_2 str.), 1631(C=O), 1085 (C-N). ^{1}H NMR (500 MHz, $CDCl_3$, in δ) 8.03 (d, J = 7.4 Hz, 2H), 7.71 (d, J = 6.6 Hz, 2H), 7.65 (m, 1H), 7.45-7.38 (m, 6H), 7.36-7.31 (m, 4H), 5.83 (dd, J = 12, 5.0 Hz, 1H), 3.80 (dd, J = 17.7, 12 Hz, 1H), 3.22 (dd, J = 17.7, 5.0 Hz, 1H); calculated Mass (m/z) for $C_{22}H_{18}N_2O$: 327.1497 $[M+H]^+$; HR-MS (m/z): 327.1492 $[M+H]^+$.

Computational Details

The DFT calculations were performed on an Intel (R) Core (TM) i7 computer using Gaussian-03 program package [25]. The geometry of the title compound was optimized using DFT/B3LYP method and 6-311++G(d,p) basis set [26,27]. The vibrational frequencies were calculated at the

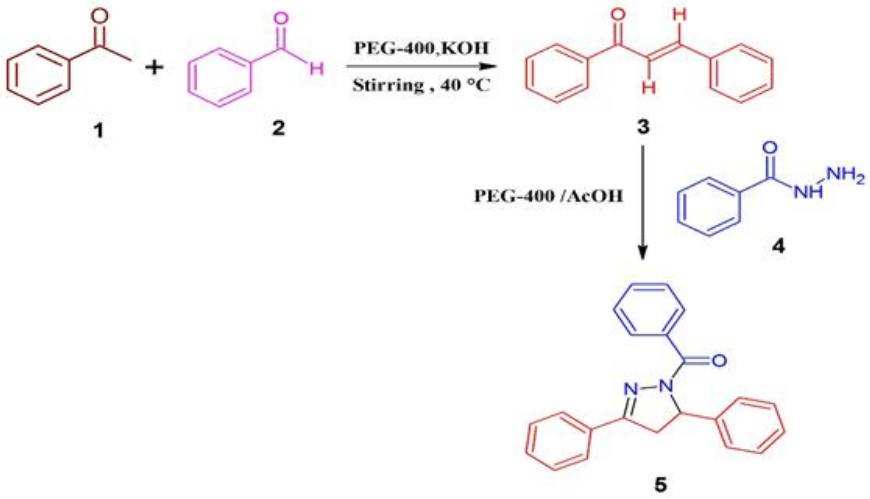

Scheme 1. Synthesis of (3,5-diphenyl-4,5-dihydro-1H-pyrazol-1-yl)(phenyl)methanone

same level of theory for the optimized structure and the obtained frequencies were scaled by scaling factor 0.9613 [28]. None of the predicted vibrational frequencies had an imaginary frequency. The UV-Vis absorption spectra of the DPPPM molecule were carried out using a TD-DFT method based on the optimized ground state structures [29]. The solvent effects were also taken into account. The HOMO-LUMO visualization and vibrational band assignments were made using the Gauss View 4.1.2 molecular visualization program [30]. From the HOMO-LUMO energies, the global reactivity parameters like electron affinity (A), ionization energy (I), chemical hardness (η), chemical softness (S), chemical potential (μ), and electrophilicity index (ω) were calculated with the help of the standard equation to investigate the reactivity and stability of the DPPPM molecule. Finally, the MESP was illustrated.

RESULTS AND DISCUSSION

Structural Studies

The optimized geometrical parameters of DPPPM molecule are given in Table 1, and optimized structures with the numbering of atoms are shown in Fig. 1. The self-consistent field energy of the DPPPM molecule at the same level and basis sets are found to be -28140.53 eV. The molecule contains a total of four rings; three are six-membered phenyl rings (ring A, B, C) and one is five-membered pyrazoline ring (p_{yz}). In pyrazoline moiety, the phenyl ring A is in the third position (C20) and the phenyl ring B is at the fifth position (C14). The phenyl ring C is connected to the pyrazoline ring at the first position (N21) *via* a carbonyl bridge. The bond lengths of C_{14}-C_{15} (1.5507 Å) and C20-C15 (1.516 Å) bonds in the pyrazoline ring show a single bond character and C_{19}-N_{20} (1.2876 Å) shows double bond character. The C-H bond length of ring lies in the range of 1.0852-1.0828 Å. The bond lengths of N-N and C_1-O_2 (C=O) bonds are computed at 1.3766 Å and 1.2238 Å, respectively. The dihedral angles N_{21}-C_{14}-C_{33}-C_{34} (133.86°) and C_{15}-C_{14}-C_{33}-C_{34} (-111.34°) indicate that the molecule is non-planer.

UV-Vis Studies

The absorption energies (λ in nm), oscillator strength (*f*) and electronic transitions of the DPPPM molecule were computed at the TD-DFT-B3LYP/6-311++G(d,p) level of theory for the optimized structure. The absorption energies (λ in nm), oscillator strength (*f*) and transitions of DPPPM molecule and experimental UV-Vis spectral analysis are given in Table 2. The theoretical UV-Vis absorption results were simulated up to three singlet excited states. The experimental UV-Vis spectra were recorded in the DCM and DMSO solvents. Likewise, the theoretical UV-Vis spectra were computed in the gas phase, DCM and the DMSO solvent. The theoretical and experimental UV-Vis

Table 1. Selected Geometrical Parameters of the Title Molecule Calculated at B3LYP/6-311++G(d,p) Level

Connectivity	Bond distance (Å)	Connectivity	Bond distance (Å)
C1-O2	1.2238	C23-H26	1.0837
C5-H9	1.0829	C24-H28	1.0828
C6-H11	1.0840	C25-H30	1.0841
C8-H12	1.0842	C27-H31	1.0843
C10-H13	1.0844	C29-H32	1.0841
C14-C15	1.5507	C34-H37	1.0849
C14-H16	1.0911	C35-H39	1.0852
C15-H17	1.0926	C36-H41	1.0843
C15-H18	1.0933	C14-N21	1.4894
C15-C20	1.5160	C1-N21	1.3844
N19-C20	1.2876	C38-H42	1.0844
N19-N21	1.3766	C40-H43	1.0842
Connectivity	Bond angle (°)	Connectivity	Bond angle (°)
O2-C1-C3	121.5	C1-N21-N19	123.4
O2-C1-N21	118.0	C14-N21-N19	113.3
C3-C1-N21	119.6	N21-C14-C33	112.7
C15-C14-N21	101.2	C15-C14-C33	114.2
C20-N19-N21	109.5	C20-C22-C23	124.4
N19-C20-C22	121.8	C20-C22-C24	120.0
C1-N21-C14	120.8	C14-C33-C35	120.9
Connectivity	Dihedral angle (°)	Connectivity	Dihedral angle (°)
N21-C1-C3-C4	-31.74	C15-C20-C22-C24	176
N21-C1-C3-C5	152.84	C15-C20-C22-C23	-3.15
O2-C1-N21-C14	0.29	C20-N19-N21-C1	-162
O2-C1-N21-N19	160.5	C20-N19-N21-C14	-0.4
C15-C14-C33-C34	-111.3	N21-N19-C20-C15	0.83
N21-C14-C33-C34	133.86	N19-C20-C22-C23	177
N21-C14-C33-C35	-48.00	N19-C20-C22-C24	-2.9

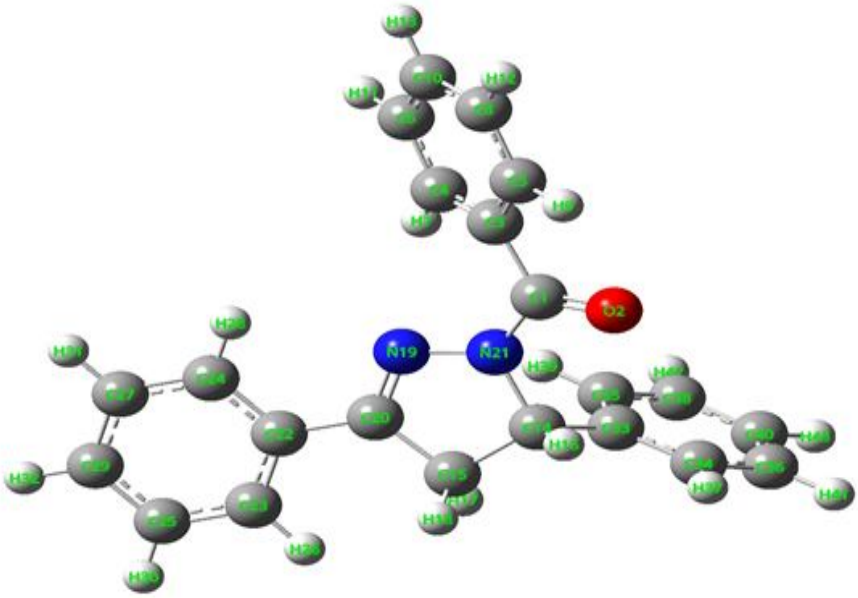

Fig. 1. Optimized structure of the title DPPPM molecule.

Table 2. Absorption Energies (λ in nm), Oscillator Strength (*f*) and Transitions of DPPPM Computed at the TD-DFT B3LYP/6-311++G(d,p) Level of Theory and Experimental UV-Vis Wavelength (Given in Brackets and Made Bold)

State	Gas-phase			DCM			DMSO		
	Config.	f	λ (nm)	Config.	f	λ (nm)	Config.	f	λ nm)
I	86 -> 87	0.5681	313.81	86 -> 87	0.6729	320.33 (301)	86 -> 87	0.6646	320.46 (303)
II	80 -> 87 80 -> 88 84 -> 87 85 -> 87 85 -> 88 86 -> 88	0.0060	284.33	86 -> 88	0.0732	283.27	86 -> 88	0.0833	283.75
III	85 -> 87 86 -> 88 86 -> 89	0.0438	279.54	79 -> 87 80 -> 87 80 -> 88 83 -> 87 84 -> 87 85 -> 87	0.0169	276.81	79 -> 87 79 -> 88 83 -> 87 84 -> 87 85 -> 87	0.0141	275.69

Config. -Configuration.

spectral images are depicted in Fig. 2. The first singlet state (S_1) is found to be at 313.81 nm in the gas phase (Fig. 2A) 320.33 nm in DCM (Fig. 2B) and 320.46 nm in DMSO (Fig. 2C). The experimental UV-visible absorption bands are centered at 301 and 303 nm in DCM (Fig. 2D) and DMSO (Fig. 2E) solvents, respectively. This result suggests that the theoretical UV-Vis absorption results are in acceptable concurrence with the UV-Vis absorption experimental results. The HOMO-LUMO electronic transition corresponds to the 86 -> 87 configurations. The solvent effect on the HOMO-LUMO absorption wavelength of the DPPPM molecule is found to be a redshift (bathochromic shift) as per the UV-Vis absorption theoretical data. The increase in the UV-Vis absorption wavelength is more in DMSO as compared to DCM. This is ascribed to the increased polarity of the DCM solvent compared to DMSO. The second singlet excited state (S_2) is present at 284.33 nm (gas phase), 283.27 nm (DCM) and at 283.75 nm (DMSO) on the theoretical UV-Vis absorption spectrum. The second gas phase singlet excited state is composed of six configurations, namely 80 -> 87, 80 -> 88, 84 -> 87, 85 -> 87, 85 -> 88 and 86 -> 88 configurations.

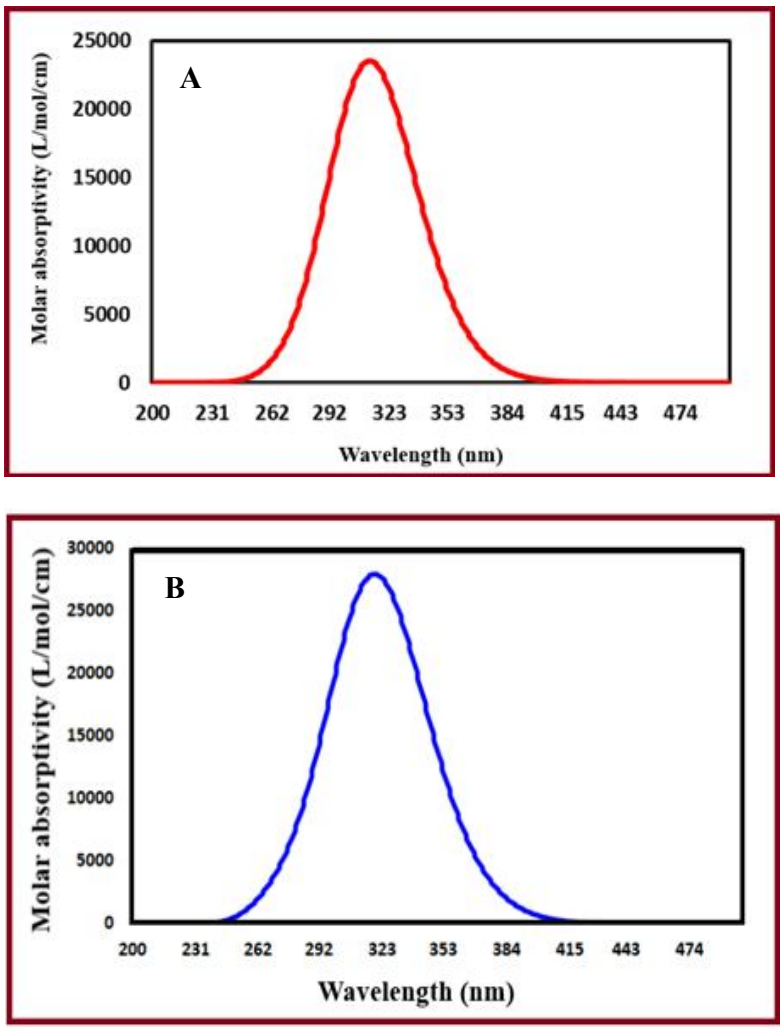

Fig. 2. Figures 2 A, B and C show the UV-Vis spectra at the B3LYP/6-311++ G(d,p) level of theory in the gas phase, in DCM and DMSO solvents, respectively. D and E are experimental UV-Vis spectra in DCM and DMSO, respectively.

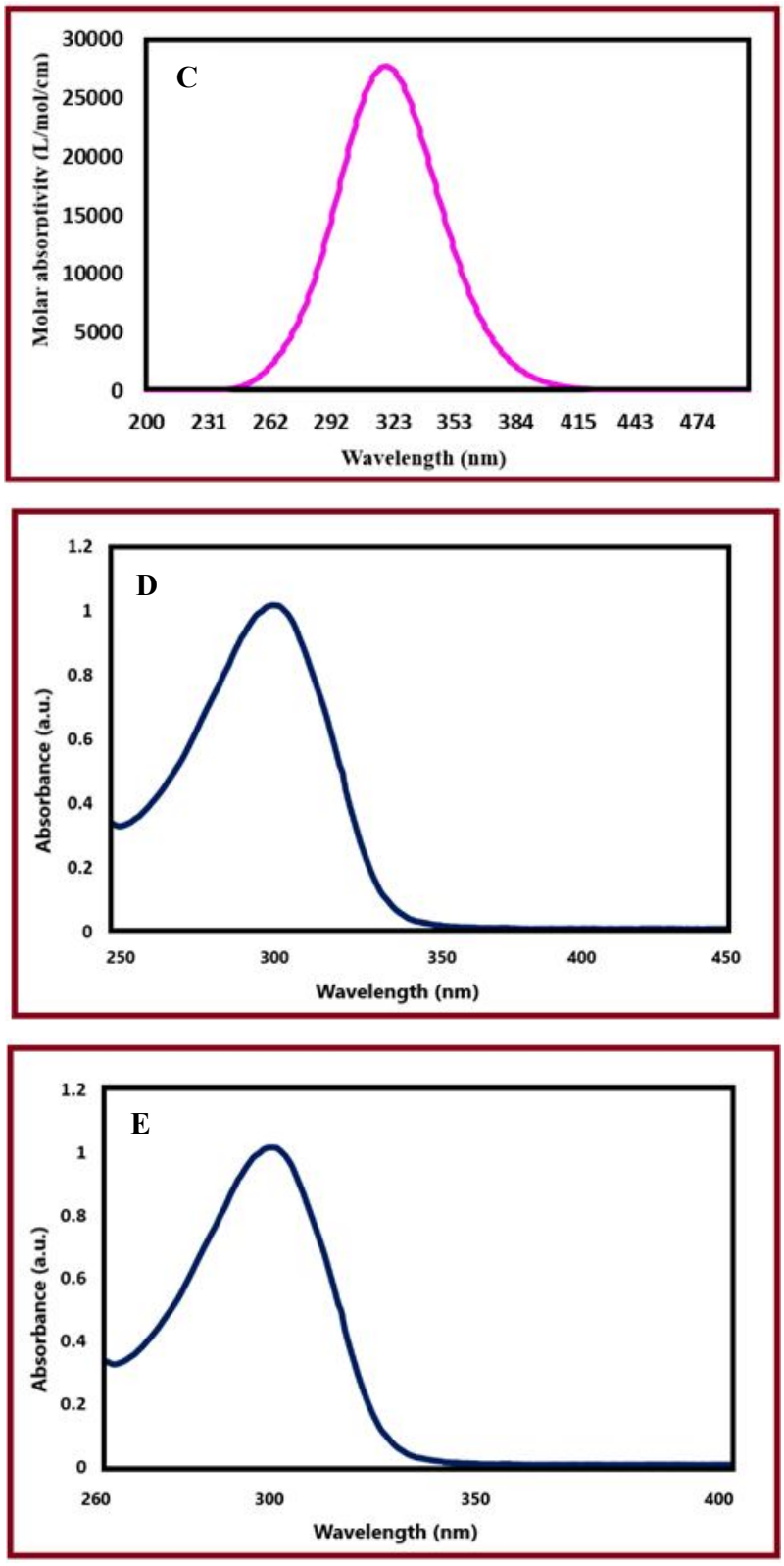

Fig. 2. Continued.

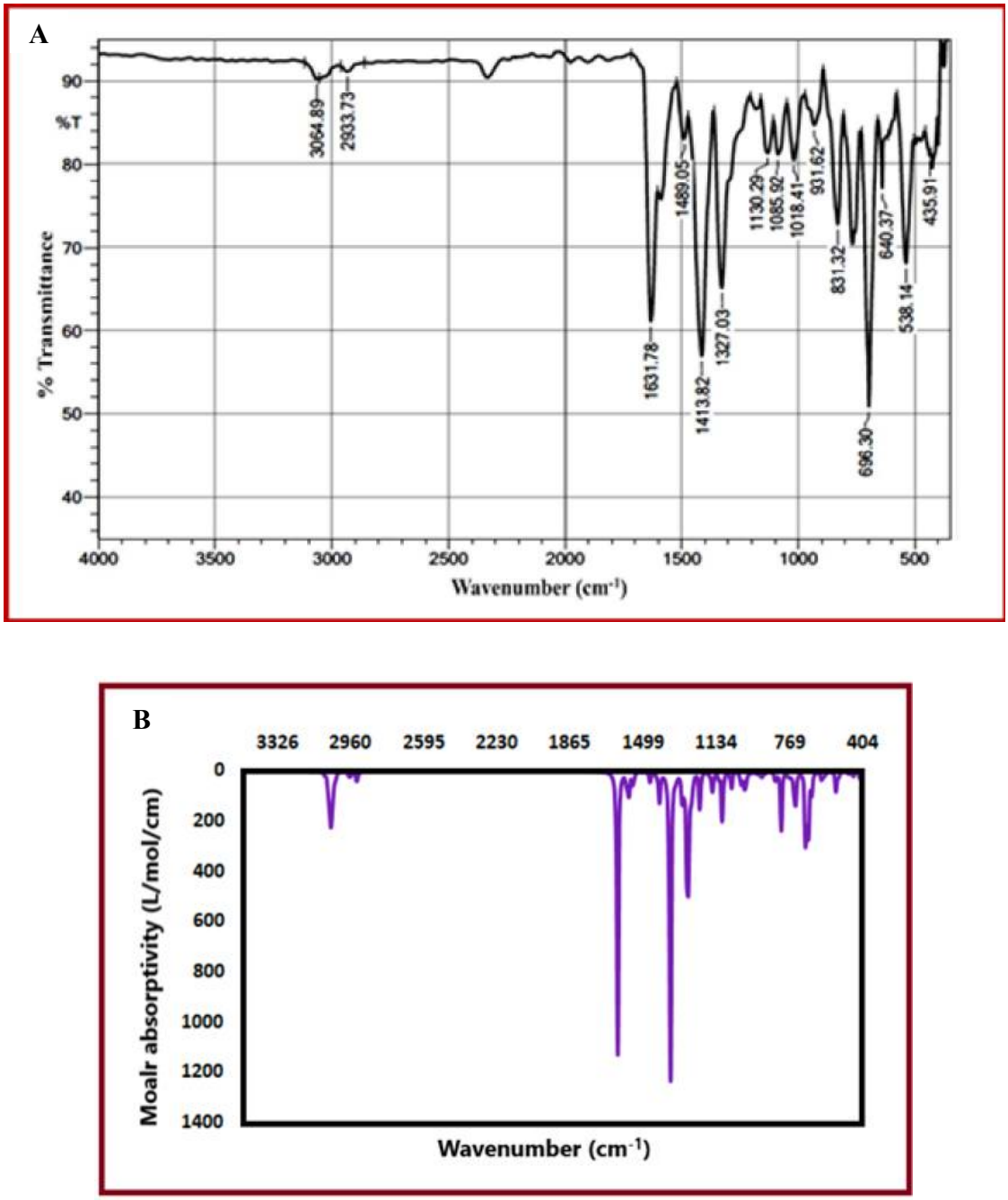

Fig. 3. (A) Experimental FT-IR spectrum of DPPPM molecule. (B) Theoretical IR spectrum of DPPPM molecule.

The third gas phase singlet excited state (S_3) is from three configurations, namely 85 -> 87, 86 -> 88, and 86 -> 89. The third absorption band is located at 279.54 nm (gas phase), 276.81 nm (DCM) and 275.69 nm (DMSO).

Vibrational Assignments

The experimental FT-IR spectrum was recorded in the region of 4000-400 cm^{-1} (solid phase) and is shown in Fig. 3A. The molecule possesses C1 point group symmetry.

Table 3. The Observed FT-IR and Calculated (B3LYP/6-311++G Level) Frequencies along with their Selected Assignments of the Title Molecule

Vibrational mode	Scaled IR frequencies (cm^{-1})	Intensity	Experimental IR frequencies (cm^{-1})	Assignments
119	3066	16.54	3064	υ C-H phenyl ring
106	2929	16.38	2933	υ CH_2 (Pyz.)
105	1629	367	1631	υ C=0
104	1584	14.3	-	υ C=N (Pyz.) + υ C=C (Ring)
97	1471	0.27	1489	υ CC (Ring a) + β CH (Ring a)
91	1418	8.08	1413	β CH (Ring c)
89	1337	7.36	1327	β CH (Pyz.) + β CH (Ring b)
80	1217	49.4	1220	β CH_2 (Pyz.) + υ C20-C22
72	1136	0.99	1130	β CH (Ring b)
70	1106	69.8	1085	υ CN (Pyz.)
66	1015	11.5	1018	υ CC (Ring a) + β CH (Ring a)
52	934	3.46	931	γ CH_2 Pyz.
47	840	18.98	831	Pyz. ring deformation
38	690	83.02	696	γ CH (Ring c)
33	659	23.05	640	T CCCC (Ring c)
27	539	22.8	538	γ CH (Ring b)
23	419	8.74	435	T CCCC (Ring b)

υ-stretching; asym-asymmetric; sym-symmetric; def-deformation; β-in-plane bending; γ-out of plane bending, Γ-torsion, Pyz-pyrazoline ring.

There are 43 atoms in the title molecule corresponding to 123 fundamental modes of vibrations. The selected theoretical (scaled) and experimental vibrational wavenumbers (in cm^{-1}) with their assignment are given in Table 3, and the simulated spectrum is shown in Fig. 3B. The Gauss-view program was used to assign the calculated harmonic vibrational wavenumbers. The aromatic C-H stretching vibrations are normally seen in the region above 3100-3000 cm^{-1} [31]. In the present case, the aromatic C-H stretching vibrations experimentally observed at 3064 cm^{-1} show a good correlation with the calculated vibrations at 3066 cm^{-1} (mode 119). The in-plane C-H bending vibrations for aromatic ring that were experimentally observed at 1489, 1413, 1327, 1130, 1018 cm^{-1} (Table 3) show a good correlation with computed vibrations at 1471, 1418, 1337, 1136 and 1015 cm^{-1}. Similarly, the out of plane vibrations

for aryl rings observed at 696,538 cm^{-1} were in agreement with computed 690,539 cm^{-1} infrared vibrations. The CH_2 group stretching vibrational mode in pyrazoline ring was computed at 2929 cm^{-1} (mode 106), and in recorded spectra, this peak was shown at 2933 cm^{-1}. The in-plane bending vibrations for the CH_2 group were observed in the spectrum at frequency 1220 cm^{-1} and theoretically was obtained at 1217 cm^{-1}. The out of plane bending vibration (rocking) for the CH_2 group was observed in the spectrum at frequency 931 cm^{-1} and theoretically was obtained at 934 cm^{-1}, showing a good correlation. On the other hand, the pyrazoline C-H in-plane bending vibration was calculated at 1337 cm^{-1} and observe at 1327 cm^{-1}. The C-N bond stretching vibrations at 1085 cm^{-1} in pyrazoline ring were confirmed by bands assigned to the calculated vibrational frequency at 1106 $cm^{-1.}$

Global Chemical Reactivity Descriptors

The highest occupied molecular orbital (HOMO) and the lowest occupied molecular orbital (LUMO) are called frontier molecular orbitals (FMOs). The TD-DFT calculations were performed in the gas phase for the frontier molecular orbitals (FMOs) to get an insight into the electronic structure of the DPPPM molecule. The frontier molecular orbitals of DPPPM are shown in Fig. 4. The HOMO represents the electron donation ability, whereas LUMO represents an electron acceptor [32]. The computed gas phase HOMO and LUMO energies were found to be -6.1375 eV and -1.8057 eV, respectively. The HOMO-LUMO energy gap was observed at 4.3318 eV. The ionization potential (I), electron Affinity (A), chemical hardness (η), chemical softness (S), electronic chemical potential (μ) and global electrophilicity index (ω) parameters were based on Koopman's theorem [33] and were calculated from equation 1-4 [34-37]. Where I and A are ionization potential and electron affinity of the compound, respectively; ($I = -\varepsilon_{HOMO}$) and ($A = -\varepsilon_{LUMO}$).

$$\eta = ½ (I - A) \quad (1)$$

$$S = 1/\eta \quad (2)$$

$$\mu = -½ (I + A) \quad (3)$$

$$\omega = \mu^2/2\eta \quad (4)$$

These parameters are used to predict the reactivity and stability of a molecule. The global reactivity parameters are listed in Table 4. The chemical hardness is a useful concept to understand the behavior of chemical systems and is associated with the stability and reactivity of a chemical system. Hard molecules having a large energy gap are more stable than soft molecules having a small energy gap. Softness (S) is a property of a molecule that measures the extent of chemical reactivity. It is the reciprocal of hardness. Soft molecules have a small HOMO-LUMO energy gap, indicating that they have small excitation energies. Therefore, electron density in a hard molecule, with a large gap, changes more hardly than a soft molecule [34]. From calculations, it was found that the DPPPM molecule is kinetically stable with the hardness (2.1659 eV) and chemical softness (0.4617 eV). The global electrophilicity index (ω) measures the capacity of a species to accept electrons [35]. The calculated chemical potential (-3.9716 eV) and the electrophilicity index (3.6413 eV) indicate that the DPPPM molecule possesses excellent chemical strength and stability.

Mulliken Atomic Charges, Molecular Electrostatic Potential and Contour Map

Milliken atomic charge calculation has an important role in the application of quantum chemical calculations to the molecular system, because of atomic charge effects dipole moment, electronic structure and some other properties of the molecular system [38,39]. The Mulliken atomic charges for DPPPM molecule are shown in Fig. 5. The Mulliken atomic charges were calculated and reported in Table 5. As indicated in Table 5, the C22 and C3 atoms carry the highest positive charge among the other carbon atoms. However, C4 and C1 atoms carry the highest negative charges amongst all carbon atoms.

MESP is a plot of electrostatic potential mapped on a constant electron density surface. The MESP is very important in studying the molecular interactions, hydrogen bonding interaction, prediction of relative sites for the nucleophilic and electrophilic attacks [40,41]. The MESP surfaces for DPPPM are shown in Fig. 6. The electrostatic potentials on the surface are represented by different colors.

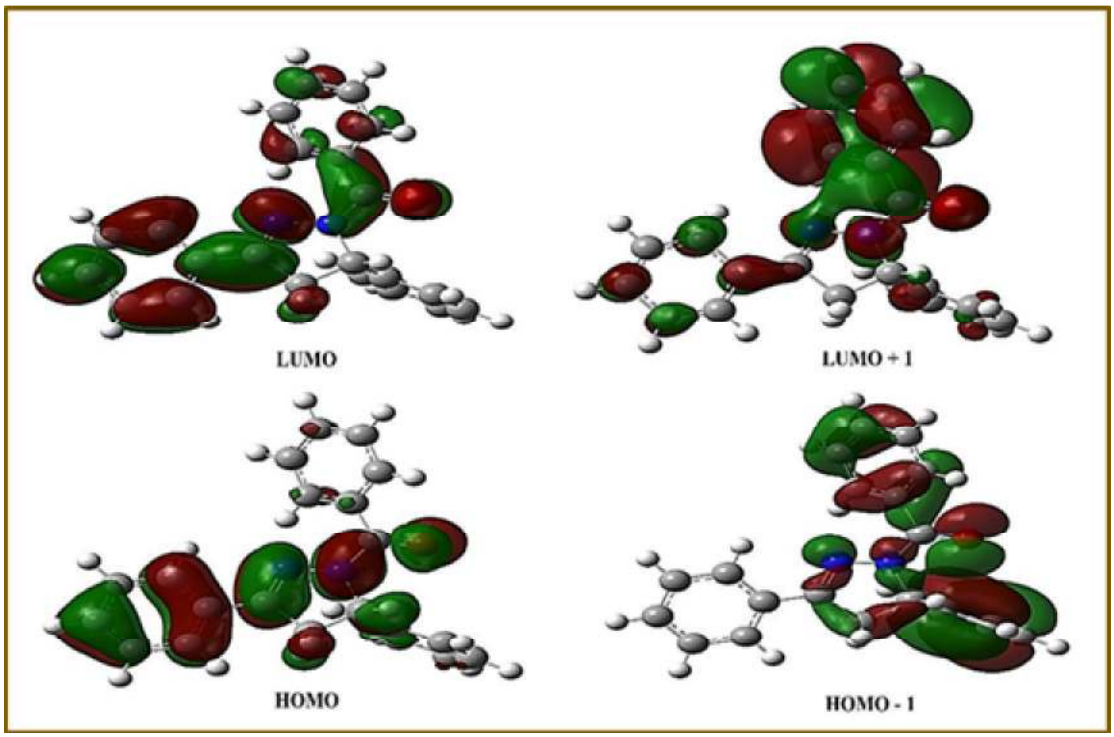

Fig. 4. The frontier molecular orbitals of the title compound obtained at the B3LYP/6-311G ++(d,p) level.

Table 4. The HOMO-LUMO Energy and Reactivity Descriptor Values of the DPPPM Molecule Calculated in the Gas Phase

Molecular properties	GAS
E_{LUMO} energy (eV)	-1.8057
E_{HOMO} energy (eV)	-6.1375
E_{LUMO+1} energy (eV)	-1.1500
E_{HOMO-1} energy (eV)	-6.8948
$\Delta E = E_{LUMO} - E_{HOMO}$ energy gap (eV)	4.3318
Electron affinity A	1.8057
Ionization energy I	6.1375
Chemical hardness η (eV)	2.1659
Chemical softness S $(eV)^{-1}$	0.4617
Chemical potential μ (eV)	-3.9716
Electrophilicity index ω (eV)	3.6413

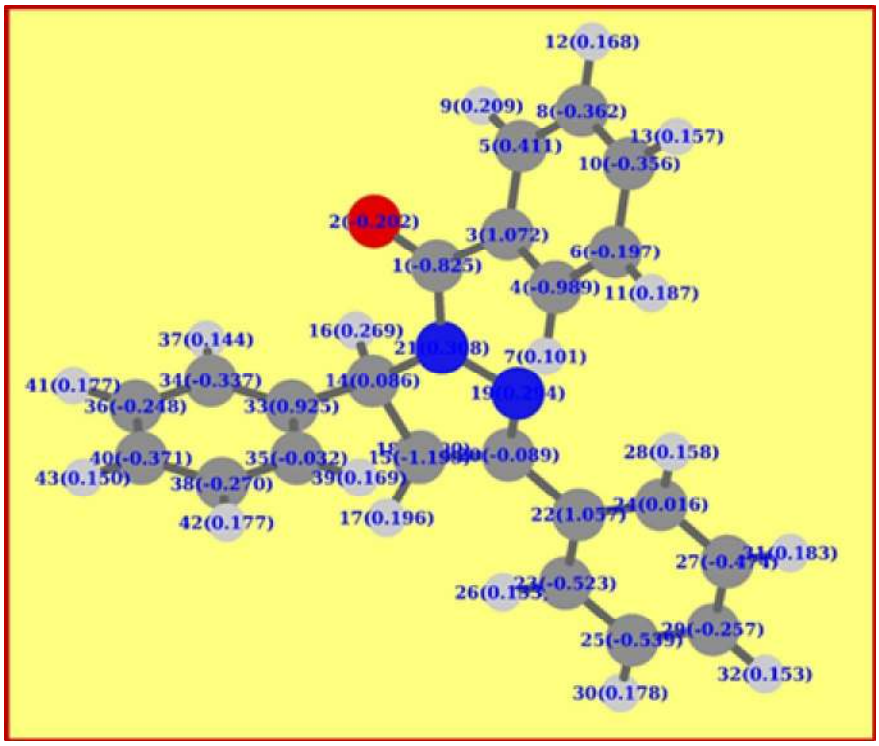

Fig. 5. Mulliken atomic charges for DPPPM.

Table 5. Mullikan Atomic Charges for the Title Compound at the B3LYP/6-311++G(d,p) Level

Atom	Charge	Atom	Charge
1C	-0.824908	22C	1.057226
2O	-0.201682	23C	-0.389743
3C	1.072497	24C	0.173368
4C	-0.88850	25C	-0.361047
5C	0.619348	27C	-0.291096
6C	-0.009996	29C	-0.103747
8C	-0.194179	33C	0.924879
10C	-0.198824	34C	-0.192645
14C	0.355453	35C	0.137202
15C	-0.812709	36C	-0.070483
19N	0.293636	38C	-0.093050
20C	-0.088941	40C	-0.220441
21N	0.308388		

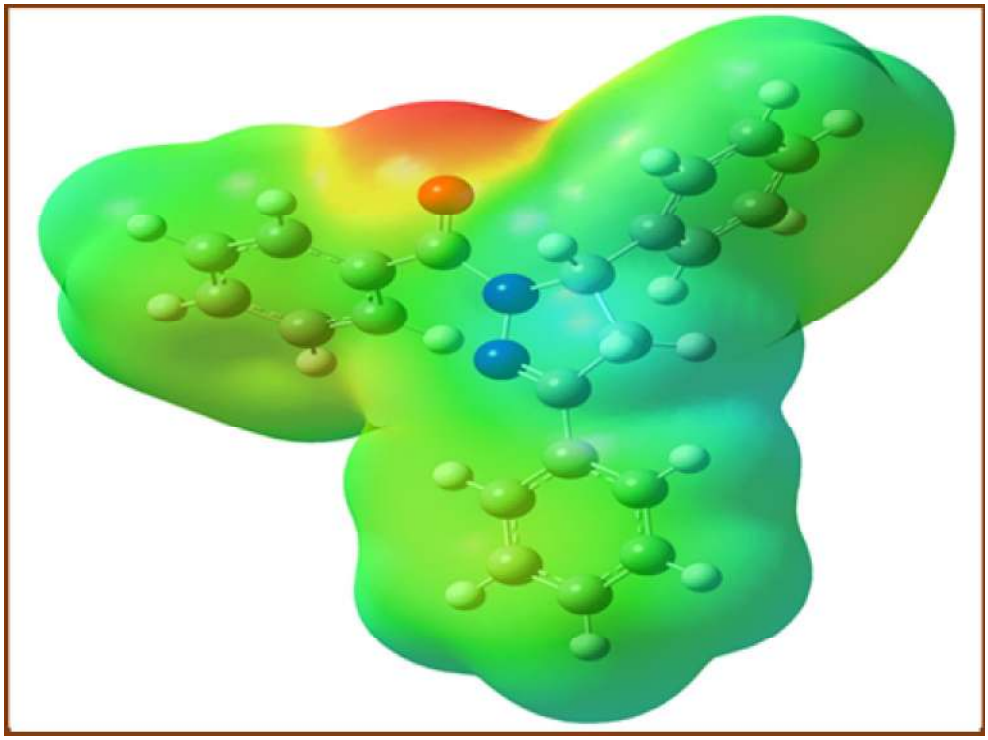

Fig. 6. Molecular electrostatic potential for DPPPM.

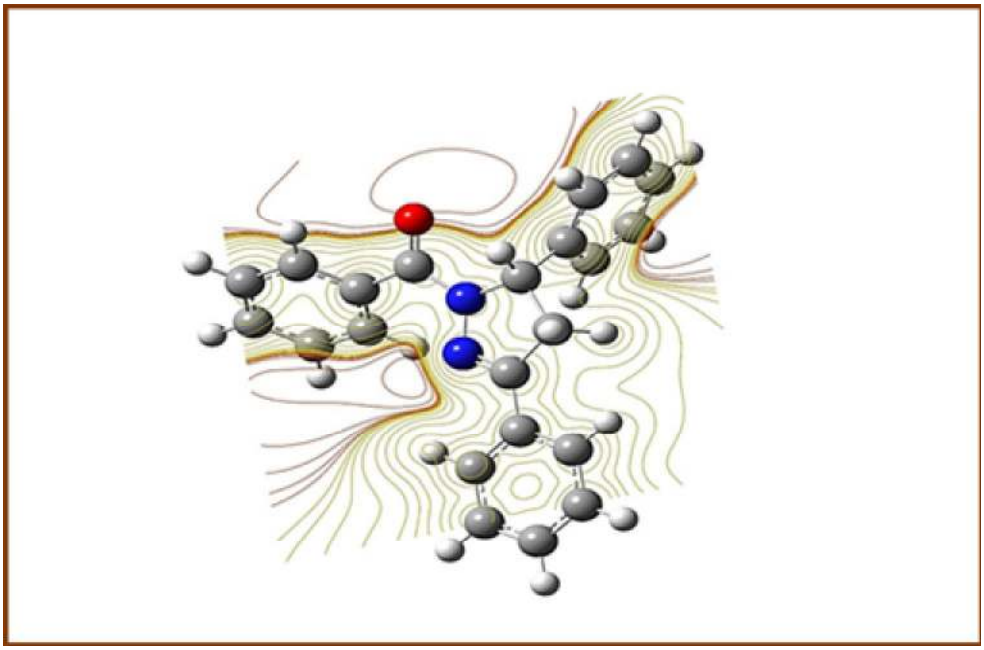

Fig. 7. Contour plot for DPPPM molecule.

The red, blue and green colours represent the regions of negative, positive and zero electrostatic potential, respectively. The negative regions V (r) was related to electrophilic reactivity (H acceptor) and the positive ones to nucleophilic reactivity (H donor). As seen in MESP surfaces, the negative electrostatic potential (red in color) is seen over the carbonyl group. So, the carbonyl group has more reactivity towards electrophile (H acceptor). The region of positive electrostatic potential (blue area) is localized over the hydrogen atoms. The electrostatic chemical potential for the DPPPM molecule is represented by a contour plot in Fig. 7.

CONCLUSIONS

We reported a simple, efficient and environmentally benign methodology for the synthesis of (3,5-diphenyl-4,5-dihydro-1*H*-pyrazol-1-yl)(phenyl)methanone. For doing so, we used PEG-400 as a readily available non-ionic liquid solvent with low cost and recyclable property. The catalytic amount of acetic acid was used to enhance the rate of intramolecular cyclization. The methodology had a simple and convenient workup procedure without use of any major equipment. We also explored various structural, chemical, electronic, and spectroscopic properties of the DPPPM molecule using the DFT method at the B3LYP/6-311++G(d,p) and TD-DFT at B3LYP/6-311++G(d,p) levels of theory. The structural investigations indicated that the DPPPM molecule is non-planar with C1 point group symmetry. The comparisons between the calculated and the experimental UV-Vis absorption spectra disclosed that the wavelength of absorption increases (red shift) with the polarity of the solvent. The correct vibrational band assignments were made by correlating scaled vibrational values with the experimental IR values. Various quantum chemical parameters were calculated to analyze the chemical behavior of the molecule. This analysis suggested that the DPPPM molecule possesses good chemical strength and stability. From the MESP, it is evident that the negative electrostatic potential regions are mainly localized over the carbonyl group, suggesting that it could be a potential site for an electrophilic attack. The overall simulated results for different molecular properties of the title compound were obtained for the first time, and we hope that they are helpful in designing new applications.

ACKNOWLEDGEMENTS

The Authors acknowledge the central instrumentation facility (CIF), Savitribai Phule Pune University, Pune and KTHM College Nashik for the spectral analysis. The authors are also grateful to Ex-Professor Dr. A. B. Sawant for the Gaussian study. Dr. Apoorva P. Hiray Coordinator, M. G. Vidyamandir institute is gratefully acknowledged for the Gaussian package.

REFERENCES

[1] Fioravanti, R.; Bolasco, A.; Manna, F.; Rossi, F.; Orallo, F.; Ortuso, F.; Alcaro, S.; Cirilli, R., Synthesis and biological evaluation of N-substituted-3,5-diphenyl-2-pyrazoline derivatives as cyclooxygenase (COX-2) inhibitors. *Euro. J. Med. Chem.* **2010**, *45*, 6135-6138, DOI: 10.1016/j.ejmech.2010.10.005.

[2] Rani, M.; Yusuf, M.; Khan, S. A.; Sahota, P. P.; Pandove, G., Synthesis, studies, and *in vitro* antibacterial activity of N-substituted-5-(furan-2-yl)-phenyl pyrazolines. *Arab. J. Chem.* **2011**, *8*, 174-180, DOI: 10.1016/j.arabjc.2010.10.036.

[3] Deng, H.; Yu, Z. Y.; Shi, G. Y.; Carabjc. J.; Tao, K.; Hou, T. P., Synthesis and *in vitro* antifungal evaluation of 1,3,5-trisubstituted-2-pyrazoline derivatives. *Chem. Biology & Drug Design* **2012**, *79*, 279-289, DOI: 10.1111/j.1747-0285.2011. 01308. x.

[4] Amir, M.; Kumar, H.; Khan, S. A., Synthesis and pharmacological evaluation of pyrazoline derivatives as new anti-inflammatory and analgesic agents. *Bioorg. Med. Chem. Lett.* **2008**, *18*, 918-922, DOI: 10.1016/j.bmcl.2007.12.043.

[5] Sridhar, S.; Rajendraprasad, Y., Synthesis and analgesic studies of some new 2-pyrazolines. *E-J. Chem.* **2012**, *9*, 1810-1815, DOI: 10.1155/ 2012/476989.

[6] Prasad, Y. R.; Rao, A. L.; Prasoona L.; Murali, K.; Kumar, P. R., Synthesis and antidepressant activity of some 1,3,5-triphenyl-2-pyrazolines and 3-(2″-hydroxy naphthalene-1″-yl)-1,5-diphenyl-2-pyrazolines. *Bioorg. Med. Chem. Lett.* **2005**, *15*, 5030-5034, DOI:

10.1016/j.bmcl.2005.08.040.

[7] Manna, F.; Chimenti, F.; Fioravanti, R.; Bolasco, A.; Secci, D.; Chimenti, P.; Ferlini, C.; Scambia, G., Synthesis of some pyrazole derivatives and preliminary investigation of their affinity binding to P-glycoprotein. *Bioorg. Med. Chem. Lett.* **2005**, *15*, 4632-4635, DOI: 10.1016/j.bmcl.2005.05.067.

[8] Parmer, S. S.; Pandey, B. R.; Dwivedi, C., Anticonvulsant activity and monoamine oxidase inhibitory properties of 1,3,5-trisubstituted pyrazolines. *J. Pharm. Sci.* **1974**, *63*, 1152-1155, DOI: 10.1002/jps.2600630730.

[9] Wang, S. Q. ; Wu, Q. H.; Wang, H. Y.; Zheng, X. X.; Shen, S. L.; Zhang, Y. R.; Miao, J. Y.; Zhao, B. X., Novel pyrazoline-based fluorescent probe for detecting glutathione and its application in cells. *Biosensor and Bioelectronics* **2014**, *55*, 386-390, DOI: 10.1016/j.bios.2013.12.047.

[10] De Silva, A. P.; Gunaratne, H. Q. N.; Gunnlaugsson, T.; Huxley, A. J. M.; McCoy, C. P.; Rademacher, J. T.; Rice, T. E., Signaling recognition events with fluorescent sensors and switches. *Chem. Rev.* **1997**, *97*, 1515-1566, DOI: 10.1021/cr960386p.

[11] Reddy, V. M.; Kim, S. J.; Lim, K. T.; Tae J. Y., Polyethylene glycol (PEG-400): an efficient green reaction medium for the synthesis of benzo[4,5] imidazole[1,2-a]-pyrimido[4,5-d]pyrimidin-4(1H)-ones under catalyst-free conditions. *Tetrahedron Lett.* **2014**, *55*, 6459-6462, DOI: 10.1016/j.tetlet.2014.09.135.

[12] Kamal, A.; Reddy, D. R.; Rajender, A simple and green procedure for the conjugate addition of thiols to conjugated alkenes employing polyethylene glycol (PEG) as an efficient recyclable medium. *Tetrahedron Lett.* **2005**, *46*, 7951-7953, DOI: 10.1016/j.tetlet.2005.09.082.

[13] Hasaninejad, A.; Beyrati, M., Eco-friendly polyethylene glycol (PEG-400): a green reaction medium for one-pot, four-component synthesis of novel asymmetrical bis-spirooxindole derivatives at room temperature. *RSC Adv.* **2018**, *8*, 1934-1939, DOI: 10.1039/C7RA13133J.

[14] Sujatha, K.; Vedula, R. R., Polyethylene glycol (PEG-400) promoted one-pot, five-component synthesis of (E)-ethyl2-(2-((E)-2-(1-(4-methyl-2-(phenylamino) thiazol-5yl) ethylidene) hydrazinyl)-4-oxothiazol-5(4H)-ylidene) acetates. *Mol. Divers.* **2019**, *24*, 413-421, DOI: 10.1007/s11030-019-09962-3.

[15] Adole, V. A.; More, R. A.; Jagdale, B. S.; Pawar, T. B.; Chobe, S. S., Efficient synthesis, antibacterial, antifungal, antioxidant and cytotoxicity study of 2-(2-Hydrazineyl) thiazole derivatives. *Chem. Select* **2020**, *5*, 2778-2786, DOI: 10.1002/slct.201904609.

[16] Modugu, N. R.; Pittala, P. K., Polyethylene glycol (PEG-400) promoted as an efficient and recyclable reaction medium for the one-pot eco-friendly synthesis of functionalized isoxazole substituted spirooxindole derivatives. *New J. Chem.* **2017**, *41*, 14062-14066, DOI: 10.1039/C7NJ03515B.

[17] Adole, V. A.; Waghchaure, R. H.; Pathade, S. S.; Patil, M. R.; Pawar, T. B.; Jagdale, B. S., Solvent-free grindstone synthesis of four new (E)-7-(arylidene)-indanones and their structural, spectroscopic and quantum chemical study: a comprehensive theoretical and experimental exploration. *Mol. Simul.* **2020**, *46*, 1045-1054, DOI: 10.1080/08927022.2020.1800690.

[18] Barim, E.; Akman, F., Synthesis, characterization and spectroscopic investigation of N-(2-acetylbenzofuran-3-yl) acrylamide monomer: Molecular structure, HOMO-LUMO study, TD-DFT and MEP analysis. *J. Mol. Struct.,* **2019**, *1195*, 506-513, DOI: 10.1016/j.molstruc.2019.06.015.

[19] Perumalsamy, R.; Kaviyarasu, K.; Nivetha, S.; Ayeshamariam, A.; Punithavelan, N.; Letsholathebe, D.; Ramalingam, G.; Jayachandran, M., Preparation, characterization and structure prediction of In_2SnO_3 and spectroscopic (FT-IR, FT-Raman, NMR and UV-Vis) study using computational approach. *J. Nanosci. Nanotechnol.* **2019**, *19*, 3511-3518, DOI: 10.1166/jnn.2019.16097.

[20] Adole, V. A..; Pawar, T. B.; Jagdale, B. S., DFT computational insights into structural, electronic and spectroscopic parameters of 2-(2-hydrazineyl) thiazole derivatives: A concise theoretical and

experimental approach. *J. Sulphur Chem.* **2020**, 1-18, DOI: 10.1080/17415993.2020.1817456.

[21] Dhonnar, S. L.; Jagdale, B. S.; Sawant, A. B.; Pawar, T. B.; Chobe, S. S., Molecular structure, vibrational spectra and theoretical HOMO-LUMO analysis of (E)-3,5-dimethyl-1-phenyl-4-(p-tolyldiazenyl)-1H-pyrazole by DFT method. *Der. Pharma. Chemica* **2016**, *8*, 119-128.

[22] Sadgir, N. V.; Dhonnar, S. L.; Sawant, A. B.; Jagdale, B. S., Synthesis, spectroscopic characterization, XRD crystal structure, DFT and antimicrobial study of (2E) -3-(2,6-dichlorophenyl)-1-(4-methoxyphenyl)-prop-2-en-1-one. *SN Appl. Sci.* **2020**, *2*, 1376-1388, DOI: 10.1007/s42452-020-2923-9.

[23] Adole, V. A.; Jagdale, B. S.; Pawar T. B.; Desale, B. S., Molecular structure, frontier molecular orbitals, MESP, and UV-Vis spectroscopy studies of ethyl-4-(3,4-dimethoxyphenyl)-6-methyl-2-oxo-1,2,3,4-tetrahydropyrimidine-5-carboxylate: A theoretical and experimental appraisal. *Mat. Sci. Res. India*, Special issue, **2020**, *17*, 13-36, DOI: 10.13005/msri.17.Special-issue1.04.

[24] Sawant, A. B.; Gill, C. H.; Nirwan, R. S., Molecular structure and vibrational spectra of 2-[5-(4-chlorophenyl)-4,5-dihydro-1H-pyrazol-3-yl]phenol. *Ind. J. Pure Appl. Phys.* 2012, *50*, 38-44.

[25] Frisch, M. J. *et al*. Gaussian 03 Revision E.01, Gaussian Inc., Wallingford CT: 2004.

[26] Becke, A. D., Density-functional thermochemistry III the role of exact exchange. *J. Chem. Phys.* **1993**, *98*, 5648-5652, DOI: 10.1063/1.464913.

[27] Lee, C.; Yang, W.; Parr, R. G., Development of the Colle-Salvetti correlation-energy formula into a functional of the electron density. *Phys. Rev. B.* **1988**, *37*, 785-789, DOI: 10.1103/PhysRevB.37.785.

[28] Foresman, J. B.; Frisch, A. E., Exploring chemistry with electronic structure methods (2nd Edn. Gaussian, Inc. Pittsburgh; PA), 1996.

[29] Runge, E; Gross, E. K. U., Density-functional theory for the time-dependent system. *Phys. Rev. Lett.* **1984**, *52*, 997-1000, DOI: 10.1103/physrevlett.52.997.

[30] Dennington, R.; Keith, T.; Milan, J., Gauss View, Version 4.1.2. Semichem Inc. Shawnee Mission, KS: 2007.

[31] Roeges, N. P. G., A Guide to the Complete Interpretation of Infrared Spectra of Organic Structures. Wiley, New York, 1994.

[32] Mishra, R.; Srivastava, A.; Sharma, A.; Tandon, P.; Baraldi, C.; Gameroni, M. C., Structural, electronic, thermodynamical and charge transfer properties of chloramphenicol palmitate using vibrational spectroscopy and DFT calculations. *Spectrapchem. Acta part A: Mol. Biomed. Spectroscopy* **2013**, 101,335-342, DOI: 10.1016/j.saa.2012.09.092.

[33] Koopmans, T. A., About the assignment of wave functions and Eigen energies to the individual electrons of an atom. *Physica* **1934**, *1*, 104-133, DOI: 10.1016/S0031-8914(34)90011-2.

[34] Pearson, R. G., Absolute electronegativity and hardness: application to organic chemistry. *J. Org. Chem.* **1989**, *54*, 1423-1430. DOI: 10.1021/jo00267a034.

[35] Parr, R. G.; Sznetpaly, L. V.; Liu, S. J., Electrophilicity index. *J. Am. Chem. Soc.* **1999**, *121*, 1922-1924, DOI: 10.1021/ja983494x.

[36] Chattaraj, P. K.; Giri, S., Stability reactivity and aromaticity of compound of multivalent superatom. *J. Phys. Chem. A* **2007**, *111*, 11116-11126, DOI: 10.1021/jp0760758.

[37] Chattaraj, P. K.; Maiti S. U., Philicity: A unified treatment of chemical reactivity and selectivity. *J. Phys. Chem. A* **2003**, *107*, 1089-5639, DOI: 10.1021/jp034707u.

[38] Govindrajan, M.; Karabacak, M.; Savitha, A.; Periandy, S., FT-IR, FT-Raman, *ab initio* HF and DFT study, NBO, HOMO-LUMO and electronic structure calculation on 4-chloro-3-nitro toluene. *Spectrochima Acta Part A* **2012**, *89*, 137-148, DOI: 10.1016/j.saa.2011.12.067.

[39] Gunasekaran, S.; Kumaresan, S.; Arunbalaji, R.; Anand, G.; Srinivasan, S., Density functional theory study of vibrational spectra and assignment of fundamental modes of dacarbazine. *J. Chem. Sci.*

2008, *120*, 315-324, DOI: 10.1007/s12039-008-0054-8.

[40] Murray, J. S; Sen, K., Molecular Electrostatic, Potentials Concepts and Applications, Elsevier, Amsterdam, 1996.

[41] Scrocco, E.; Tomasi, J., Electronic molecular structure, reactivity, and intermolecular forces: An euristic interpretation by means of electrostatic molecular potentials. *Adv. Quantum Chem.* **1978**, *11*, 115-193, DOI: 10.1016/S0065-3276 (08)60236-1.